

# Novel Biocompatible Polysaccharide-Based Self-Healing Hydrogel

Zhao Wei, Jian Hai Yang, Zhen Qi Liu, Feng Xu, Jin Xiong Zhou, Miklós Zrínyi, Yoshihito Osada, and Yong Mei Chen\*

A novel biocompatible polysaccharide-based self-healing hydrogel, CEC-I-OSA-I-ADH hydrogel ("I" means "linked-by"), is developed by exploiting the dynamic reaction of *N*-carboxyethyl chitosan (CEC) and adipic acid dihydrazide (ADH) with oxidized sodium alginate (OSA). The self-healing ability, as demonstrated by rheological recovery, macroscopic observation, and beam-shaped strain compression measurement, is attributed to the coexistence of dynamic imine and acylhydrazone bonds in the hydrogel networks. The CEC-I-OSA-I-ADH hydrogel shows excellent self-healing ability under physiological conditions with a high healing efficiency (up to 95%) without need for any external stimuli. In addition, the CEC-I-OSA-I-ADH hydrogel exhibits good cytocompatibility and cell release as demonstrated by three-dimensional cell encapsulation. With these superior properties, the developed hydrogel holds great potential for applications in various biomedical fields, e.g., as cell or drug delivery carriers.

## 1. Introduction

As one of the most attractive soft materials with 3D network structure and tunable physical and chemical properties mimicking natural extracellular matrices, hydrogels find widespread applications in various biomedical fields, e.g., as scaffolds for tissue engineering, and as delivery vehicles for cells, drugs, proteins, or genes.<sup>[1–8]</sup> Recently, self-healing hydrogels capable of autonomously repairing cracks, offer substantial benefits to

maintain the integrity of network structures and mechanical properties of bulk gels, leading to their long-term use with stable functionality.<sup>[9–13]</sup>

The scientific community nowadays focus on two major approaches, based on dynamic covalent bond<sup>[14–17]</sup> and non-covalent bond,<sup>[18–28]</sup> to design self-healing hydrogels. Dynamic covalent bond integrates both the stability of covalent bond and the reversibility of noncovalent bond in one system.<sup>[29]</sup> These dynamic covalent bonds can build an intrinsic dynamic equilibrium of bond generation and dissociation in hydrogel networks, endowing self-healing performance to the hydrogels. Despite a few examples of self-healing hydrogels based on the dynamic covalent bonds (e.g., phenylboronate esters,<sup>[30–32]</sup> acylhydrazone bonds,<sup>[29,33]</sup> disulfide

bonds,<sup>[34–36]</sup> and Diels-Alder reactions,<sup>[37,38]</sup> the difficulty of manipulating *in vivo* due to their nonautonomous self-healing characteristics, impedes their applications. For instance, self-healing hydrogel based on dynamically restructuring of phenylboronic esters needs an acid environment (pH 4.2),<sup>[30]</sup> while hydrogel based on dynamic disulfide bonds usually needs an alkali environment (pH 9),<sup>[34]</sup> to trigger the corresponding healing process. Moreover, complicated synthetic procedures and unconfirmed biocompatibility of these self-healing hydrogels may limit their applications. For instance, the self-healing

Z. Wei, Dr. J. H. Yang, Z. Q. Liu, Prof. Y. M. Chen  
School of Science  
State Key Laboratory for Mechanical Behaviour of Materials  
Collaborative Innovation Center of Suzhou Nano Science and Technology  
Xi'an Jiaotong University  
Xi'an 710049, ShaanXi, P.R. China  
E-mail: chenym@mail.xjtu.edu.cn

Z. Wei, Dr. J. H. Yang, Z. Q. Liu, Prof. F. Xu, Prof. Y. M. Chen  
Biospired Engineering and Biomechanics Center (BEBC)  
Xi'an Jiaotong University  
Xi'an 710049, ShaanXi, P.R. China

Prof. F. Xu  
The Key Laboratory of Biomedical Information Engineering  
of Ministry of Education  
School of Life Science and Technology  
Xi'an Jiaotong University  
Xi'an 710049, ShaanXi, P.R. China

Prof. J. X. Zhou  
State Key Laboratory for Strength  
and Vibration of Mechanical Structures  
School of Aerospace  
Xi'an Jiaotong University  
Xi'an 710049, ShaanXi, P.R. China

Prof. M. Zrínyi  
Laboratory of Nanochemistry  
Department of Biophysics and Radiation Biology  
Semelweis University  
H-1084, Budapest, Nagyvárud tér 4, Hungary

Prof. Y. Osada  
RIKEN 2-1  
Hirosawa  
Wako, Saitama 351-0198, Japan



DOI: 10.1002/adfm.201401502



Subsequently, a new absorption of imine stretching vibration ( $C=N$ ) at  $1644\text{ cm}^{-1}$  was observed, indicating that condensation reaction between CEC and OSA forms a Schiff's base.

To analyze the influence of CEC concentration on the mechanical properties of the CEC-I-OSA-I-ADH hydrogel, we measured the rheological properties of the hydrogels with different molar ratios of amino groups (from CEC) to aldehyde groups (from OSA),  $R = M-NH_2:M-CHO$  ( $0 \leq R \leq 1$ ). We controlled the concentration of hydrazide groups (from ADH), to ensure that the residual aldehyde groups completely reacted (i.e.,  $M-CHO = M-CONHNH_2 + M-NH_2$ ). As a result, when  $R$  increases, CEC and associated imine bonds concentration increases, but ADH and corresponding acylhydrazone bonds concentration reduces. Oscillatory frequency sweep experiments conducted at  $25\text{ }^\circ\text{C}$  under constant strain was used for evaluating mechanical strength of the CEC-I-OSA-I-ADH hydrogels (Figure S2, Supporting Information). The storage modulus ( $G'$ ) of the hydrogels increased steeply from  $717 \pm 113$  to  $5814 \pm 166$  Pa with  $R$  varying from 0 to 0.5, due to the significant increase of CEC with high molecular weight. The  $G'$  reached a plateau of  $6044 \pm 224$  Pa and then slightly dropped to  $5316 \pm 318$  Pa when  $R$  continuously increased from 0.5 to 1 (Figure 2a). This is probably because the concentration of more dynamic imine bonds (compared with acylhydrazone bonds) increases with  $R$ , resulting in an instable polymer networks. The CEC-I-OSA-I-ADH hydrogels with shear moduli in a range of  $10^2$ – $10^3$  Pa can potentially be used in tissue engineering for repairing soft nerve and brain tissues with similar moduli.<sup>[60]</sup>

## 2.2. Self-Healing Performance of the CEC-I-OSA-I-ADH Hydrogel

To assess the self-healing behaviors of the CEC-I-OSA-I-ADH hydrogel, we performed the rheological recovery tests with fixed  $R = 0.5$ . From the results of strain amplitude sweep of the CEC-I-OSA-I-ADH hydrogel, the  $G'$  and the loss modulus ( $G''$ ) curve intersects at the strain of 80%, indicating that the state of hydrogel is between solid and fluid near this critical point. With further increase of the strain to 800%, the  $G'$  dramatically decreased from  $\approx 5880$  Pa to  $\approx 79$  Pa due to the collapse of the hydrogel networks (Figure 2b). Based on the strain amplitude sweep results, the continuous step strain measurements were performed to test the rheology recovery behavior of the CEC-I-OSA-I-ADH hydrogel. As the oscillatory shear strain stepped from 1% to 80% and maintained for 100 s, the  $G'$  and  $G''$  overlapped, while they immediately recovered their original values after the strain back to 1% (Figure 2c). Similarly, when the larger strains (300% and 800%) and small strain (1%) were alternatively applied later, the  $G'$  also quickly restored the initial value. Moreover, fixing step strain to 800% but varying the loading period from 100 to 300 s, the effect of the duration of the breaking strain on the rheological recovery behavior was investigated thoroughly (Figure 2d). The data showed that the  $G'$  immediately recovered after the breaking strain was removed, regardless of loading period. These results suggest that polymer networks of CEC-I-OSA-I-ADH hydrogel exhibit rapid recovery when the hydrogel is subject to oscillatory shear strain.

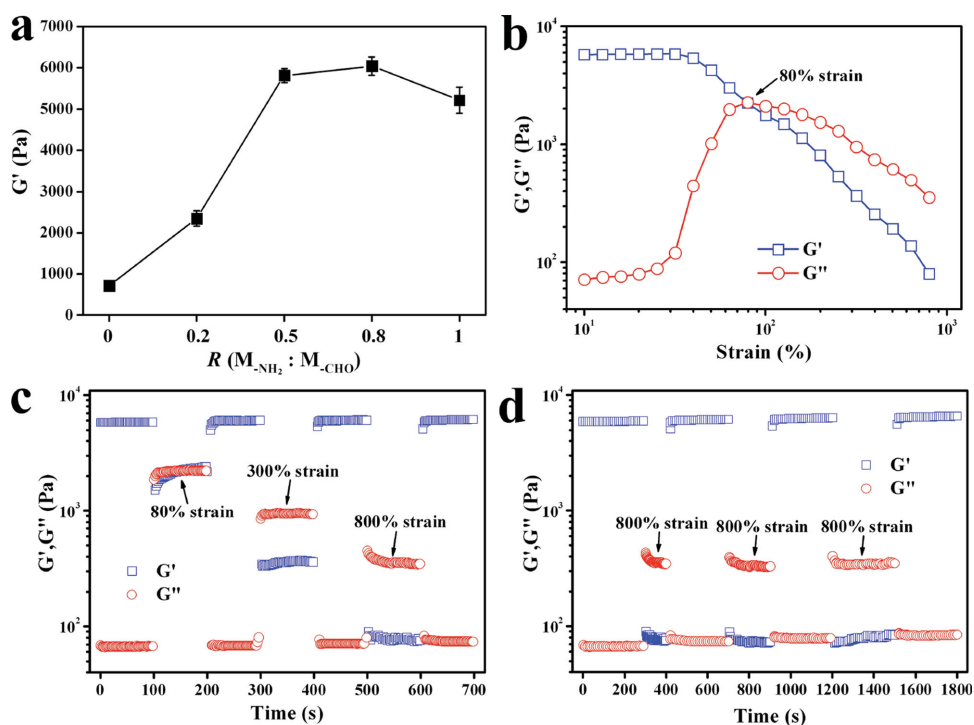


**Figure 2.** The rheological measurement of CEC-I-OSA-I-ADH hydrogel. a) The storage moduli ( $G'$ ) of CEC-I-OSA-I-ADH hydrogels with  $R = 0.2, 0.5, 0.8, 1.0$ . The data are extracted from the plateaus of variation of storage moduli versus angular frequency ( $1\text{ rad s}^{-1}$  to  $10\text{ rad s}^{-1}$ ). Error ranges are standard deviations over  $n = 3$  samples. b) The  $G'$  and  $G''$  of the hydrogel from strain amplitude sweep ( $\gamma = 10\%$ – $800\%$ ) at a fixed angular frequency ( $10\text{ rad s}^{-1}$ ). c) The  $G'$  and  $G''$  of the hydrogel when alternate step strain switched from small strain ( $\gamma = 1.0\%$ ) to large strain ( $\gamma = 80\%$ ,  $300\%$ , and  $800\%$ ) at a fixed angular frequency ( $10\text{ rad s}^{-1}$ ). Each strain interval was kept as 100 s. d) The cyclic  $G'$  and  $G''$  values of the hydrogel for a large strain level ( $\gamma = 800\%$ ) and different loading period from 100 to 300 s.

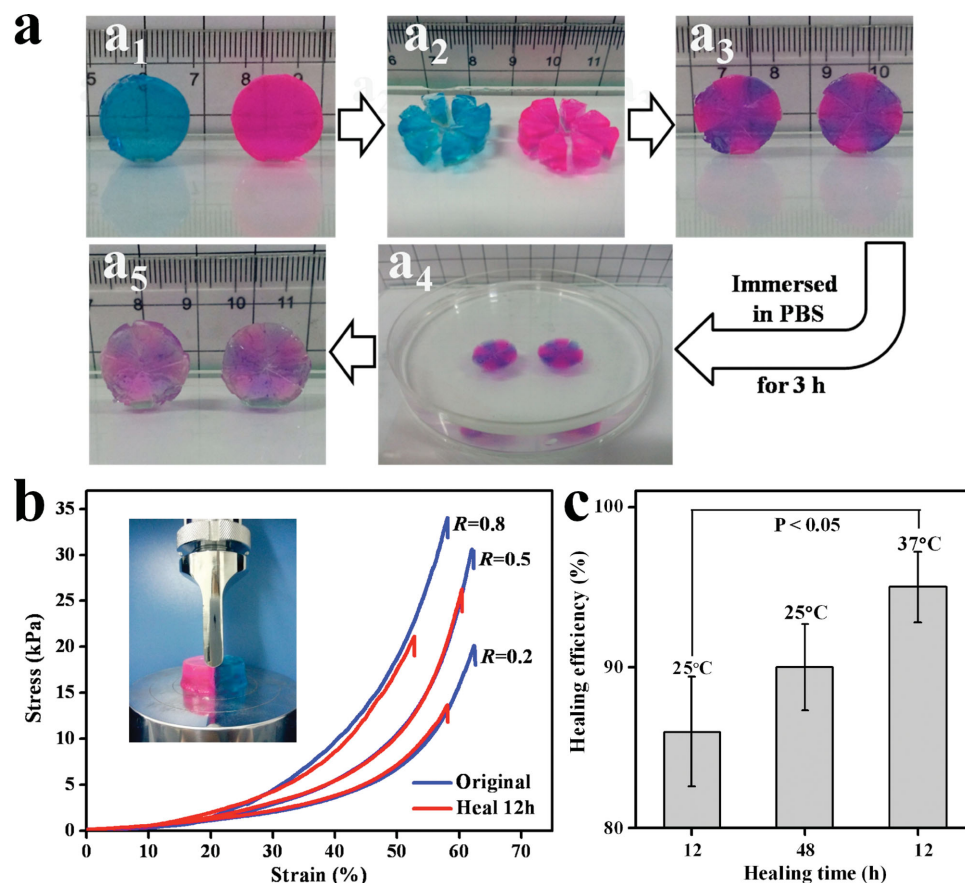


**Figure 3.** Photographs of self-healing process and beam-shaped compression test of the CEC-I-OSA-I-ADH hydrogel. a) Two disk-shaped hydrogels (one stained with rhodamine B and the other stained with methylene blue) ( $a_1$ ); hydrogels were cut into equal 8 pieces ( $a_2$ ); the self-healed hydrogel disks can stand after healing for 6 h at 25 °C without any external intervention ( $a_3$ ); after immersed in PBS (pH 7.0) for 3 h, the healed hydrogel disks can retain their shape ( $a_4, a_5$ ). b) The beamed-shape strain compression curves of the hydrogels with  $R = 0.2, 0.5, 0.8$  prepared in pH 7.0 PBS before and after healing for 12 h. c) Enhance the healing efficiency of the hydrogel ( $R = 0.5$ ) by prolonging the healing time to 48 h and increasing the healing temperature to 37 °C.  $p < 0.05$  versus healing 12 h at 25 °C. Error ranges are standard deviations over  $n = 3$  samples.

To further evaluate the self-healing ability of the CEC-I-OSA-I-ADH hydrogel ( $R = 0.5$ ), we performed macroscopic self-healing test (Figure 3a). In details, the two disk-shaped hydrogels with red (stained with rhodamine B) and blue colors (stained with methylene blue) were cut into equal 8 pieces by a razor blade, respectively (Figure 3a<sub>1,2</sub>). Subsequently, the total 16 pieces of broken hydrogels were combined into two blended integral hydrogel disks with alternate colors. After 6 h at 25 °C without any external intervention, the boundaries between the different colored pieces turned obscure, and the blended integral hydrogel disks could stand up by themselves (Figure 3a<sub>3</sub>), demonstrating the self-healing performance of the hydrogel. Moreover, the healed hydrogel disks can maintain their shape and no splitting were observed after being immersed in PBS (pH = 7.0) for 3 h (Figure 3a<sub>4,5</sub>). This reveals that dynamic reaction among the dynamic functional groups rather than the simple adhesion takes place at the interfaces of broken hydrogels. The existence of dynamic covalent bonds in the hydrogel networks is thus crucial for the self-healing behavior.

To determine the self-healing efficiency, we performed the beam-shaped strain compression test of the CEC-I-OSA-I-ADH hydrogel ( $R = 0.2, 0.5, 0.8$ ) (Figure 3b).<sup>[23,24]</sup> The healing

efficiency ( $HE$ ) is defined as the ratio of healing strength ( $S_h$ ) at breaking point of the healed sample over initial strength ( $S_i$ ) of pristine samples, i.e.,  $HE = (S_h/S_i)$ .<sup>[9]</sup> After healing for 12 h at 25 °C, the measured  $HE$  of the hydrogels was  $86 \pm 3.4\%$  when  $R = 0.5$ , while it dropped to  $68 \pm 5.2\%$  and  $62 \pm 2.7\%$  when  $R = 0.2$  and  $0.8$ , respectively. These results can be explained by the appropriate balance between the mobility of polymer chains and the dynamics of the cross-links, which both affect the self-healing performance of the hydrogels. In the case of  $R = 0.8$  sample with high CEC content, although the number of more dynamic imine bonds increased in the polymer cross-links, a large amount of CEC with high molecular weight led to poor mobility of the polymer chains due to an increased viscosity of the hydrogel system, resulting in a low  $HE$ . On the other hand, in the case of  $R = 0.2$  sample with low CEC content, although the viscosity of hydrogel system was reduced, the increased number of acylhydrazine bonds with the relatively slow exchange and equilibrium kinetics in neutral PBS at room temperature mainly limit the  $HE$ .<sup>[45–47]</sup>

Therefore, to improve the  $HE$  of the CEC-I-OSA-I-ADH hydrogel, prolonged healing time and increased temperature were adopted. In the case of  $R = 0.5$ , as expected,  $HE$

went up to  $90 \pm 2.7\%$  when the healing time was prolonged to 48 h, but there was no significant increase compared with the *HE* of 12 h. On the other hand, the *HE* can reach as high as  $95 \pm 2.2\%$  when the healing temperature increased to  $37^\circ\text{C}$  (physiological temperature) (Figure 3c). This demonstrates that the hydrogel exhibits excellent self-healing capability under physiological conditions. The *HE* of the hydrogel shows a significant increase, nearly 10%, as compared with that at room temperature, which is due to the effect that higher temperature can enhance the dynamic kinetics of the reversible bonds.<sup>[56]</sup>

Besides, to probe the effect of pH on *HE*, the weakly acidic PBS (pH 6.0) as solvent instead of neutral PBS were adopted to prepare the CEC-I-OSA-I-ADH hydrogel ( $R = 0.2, 0.5, 0.8$ ). When pH decreased to 6.0, the *HE* experienced a sharp rise to  $91\% \pm 4.5\%$  from  $68\% \pm 5.2\%$  for the  $R = 0.2$  sample, and could reach up to  $94\% \pm 4.2\%$  when  $R$  reached to 0.5 (Figure S3a,b, Supporting Information). However, when  $R$  increased to 0.8, the *HE* only slightly rose to  $69\% \pm 3.1\%$  from  $62\% \pm 2.7\%$ . The hydrogel with more acylhydrazone cross-links (low  $R$ ) exhibited a large growth of *HE*, because the weakly acid condition (pH 4–6) accelerate the dynamic exchange reaction of acylhydrazone bonds.<sup>[33,34]</sup> Moreover, the *HE* of  $R = 0.2$  and 0.5 samples are similar under pH 6.0 condition although the mobility of polymer chains in  $R = 0.2$  sample is higher than that of  $R = 0.5$  sample, because imine bonds are more dynamic than acylhydrazone bonds.

### 2.3. Injectability of the Self-Healing CEC-I-OSA-I-ADH Hydrogel

The self-healing hydrogels can also be used as injectable hydrogels for cell therapy and drug delivery.<sup>[57,58]</sup> Unlike the traditional injectable hydrogels, self-healing hydrogels have the capability to be injected after gelation. The broken hydrogel pieces squeezed from the needle can self-assemble

and self-heal into an integral hydrogel at the target site. This injectability of self-healing hydrogels has been confirmed to offer more uniform distributions of cargos (drug/cell etc.) and more controllable placement of hydrogels in vivo.<sup>[49,59]</sup> To prove the injectability of our CEC-I-OSA-I-ADH hydrogel, two pieces of hydrogel disks stained with different colors were put into needle tubing (Figure 4a,b), then injected into a 10 mL beaker and compacted in the bottom of the beaker (Figure 4c). After healing at  $25^\circ\text{C}$  for 6 h, the self-healed hydrogel disk can stand up by itself and maintain its integrity even after being immersed in PBS (pH = 7.0) for another 3 h (Figure 4d–f). Moreover, we also proved the drug release behavior of the self-healed hydrogel. The rhodamine B and methylene blue were used as two small molecular model drugs. Figure S4 (Supporting Information) plots the release curves of the two model drugs between the self-healed hydrogel and the other two prepared hydrogels. The minor difference between these curves indicates that self-healing process has nearly negligible effects on drug release ability.

### 2.4. Cytocompatibility and Cell Release of the Self-Healing CEC-I-OSA-I-ADH Hydrogel

To explore the cytocompatibility and cell release of CEC-I-OSA-I-ADH hydrogel ( $R = 0.5$ ), we perform the test of 3D encapsulation of NIH 3T3 fibroblasts. From the Live/Dead staining of cells, we found that the cell viability of NIH 3T3 fibroblasts encapsulated in CEC-I-OSA-I-ADH hydrogel was  $98.5\% \pm 1.2\%$ ,  $97.6\% \pm 4.0\%$ , and  $95.3\% \pm 3.4\%$  after 12, 24, and 48 h in vitro culture, respectively (Figure 5a,b). When cultured for 72 h, the hydrogel was partially degraded, hydrolytic degradation and enzymes produced by the cells may contribute to the degradation of the polymer networks. Then the encapsulated cells could be released from the hydrogel. We continuously cultured

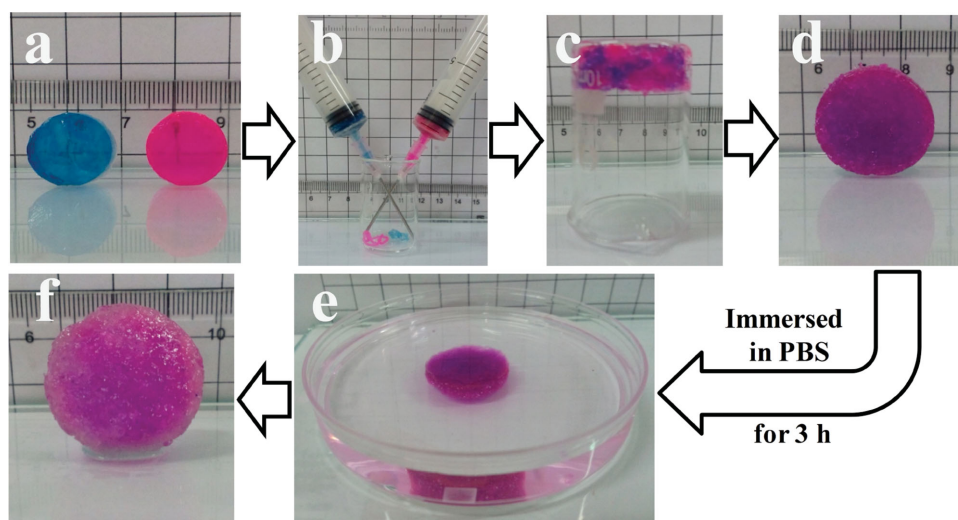


**Figure 4.** The injectable process of the self-healing CEC-I-OSA-I-ADH hydrogel ( $R = 0.5$ ). a) Two disk-shaped hydrogels (one stained with rhodamine B and the other stained with methylene blue), b,c) separately injected into a 10 mL small beaker from needles and compacted at the bottom of the beaker. d) The self-healed hydrogel disk can stand after healing for 6 h at  $25^\circ\text{C}$  without any external intervention. e,f) After immersed in PBS (pH 7.0) for 3 h, the healed hydrogel disks can maintain their integrity.

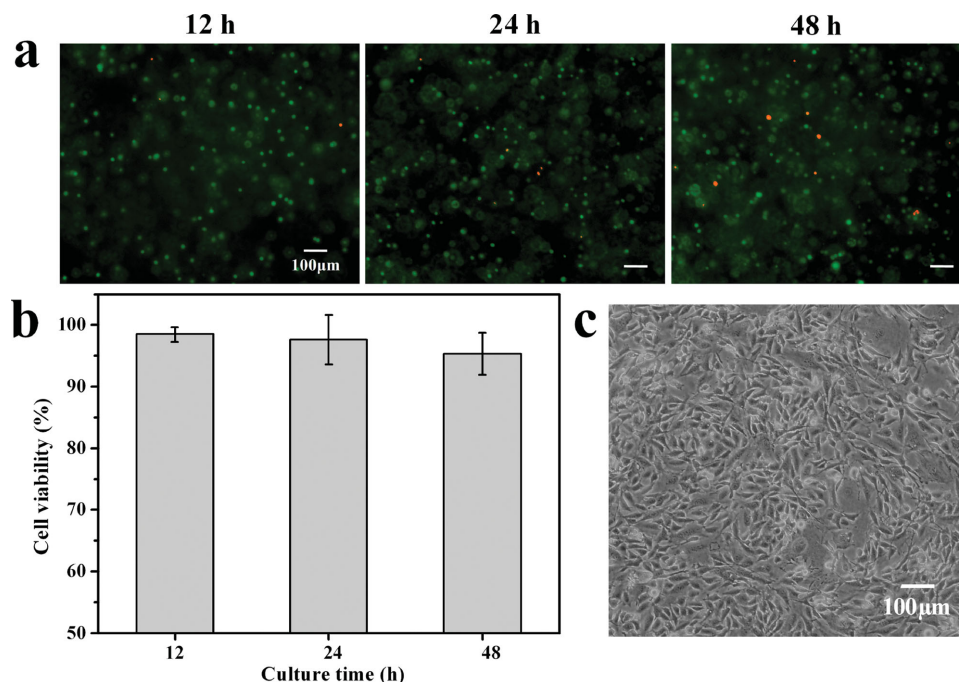


**Figure 5.** 3D cell encapsulation of the CEC-I-OSA-I-ADH hydrogel ( $R = 0.5$ ). a) Live/Dead staining of the encapsulated NIH 3T3 fibroblasts for 12, 24, and 48 h, respectively. b) The cell viability versus different culture times. c) The released NIH 3T3 cells from 3D cell encapsulation were cultured on tissue culture polystyrene plates for 3 days.

them on the tissue culture polystyrene plates for other 3 days. The released NIH 3T3 fibroblasts exhibited normal cell morphology and could proliferate with culture time (Figure 5c). The results illustrate the cytocompatibility CEC-I-OSA-I-ADH hydrogels exhibit excellent cell release behavior.<sup>[60]</sup>

### 3. Conclusion

In summary, we developed a novel polysaccharide-based self-healing CEC-I-OSA-I-ADH hydrogel. The dynamic imine and acylhydrazone bonds coexist in the hydrogel networks, enabling occurrence of dynamic reaction under mild conditions. This dynamic nature of the system imparts the self-healing capability to the hydrogel, as confirmed by the rheological recovery test, macroscopic self-healing test, and beam-shaped strain compression measurement. The healing efficiency of the CEC-I-OSA-I-ADH hydrogel can achieve 95% under physiological conditions. With the good self-healing property and cytocompatibility, the hydrogel could be potentially used as cell and drug delivery carrier as confirmed by drug release and cell encapsulation. We anticipate that this polysaccharide-based biocompatible self-healing hydrogel might offer diverse applications in biomedical fields.

### 4. Experimental Section

**Materials:** Sodium alginate (>350 mpa s), acrylic acid, and sodium periodate were purchased from Alfa Aesar. Chitosan (degree of deacetylation 86%, Mw = 200 000 Da) was from Tokyo Kasei Kogyo Co., Ltd. Methylene blue and rhodamine B (95%) were supplied by Sigma-Aldrich. All other chemicals were analytical grade and used without further purification.

**Synthesis of *N*-Carboxyethyl Chitosan (CEC):** *N*-carboxyethyl chitosan was prepared by the previous method of Michael's reaction.<sup>[53–55]</sup> Briefly, chitosan (1.0 g, 6.2 mmol) was dissolved in 50 mL distilled water containing acrylic acid (1.46 mL, 21.3 mmol), and the mixture was magnetically stirred at 50 °C for 3 days. Then the pH of the solution was adjusted to 10–12 by 1 mol L<sup>-1</sup> NaOH. Thereafter, the solution was dialyzed (MWCO 8000) against distilled water for 3 days with repeated change of water, followed by freezing dried to obtain the pure CEC powder. Typical yield of the products was ≈77%. <sup>1</sup>H NMR (400 MHz, D<sub>2</sub>O, δ): 1.94 (s, 3H, COCH<sub>3</sub>), 2.83 (s, 2H, CH<sub>2</sub>CO<sub>2</sub>Na), 3.30–4.87 (m, glucosamine). The degree of substitution was 38%, which was determined according to the <sup>1</sup>H NMR spectra by comparing the peak area of the acetamide methyl protons (δ = 1.94) in chitosan and the methylene protons (δ = 2.83) of acrylic acid in CEC.

**Synthesis of Oxidized Sodium Alginate (OSA):** The synthesis of OSA was based on a reported method with a slight modification.<sup>[42]</sup> Sodium alginate (1.0 g, 5 mmol) was dissolved in 100 mL distilled water, then sodium periodate (1.08 g, 5 mmol) was added, and the solution was magnetically stirred in the dark at 25 °C for 5 h. The reaction was terminated by adding ethylene glycol (1.5 mL) and stirring for additional 1 h. After reaction, the mixture was dialyzed (MWCO 3000) against distilled water for 3 days with repeated change of water, followed by lyophilizing to obtain the products of OSA. Typical yield of the products was ~70%.

**Determination of the Degree of Oxidation (DO):** The DO was evaluated by the iodometry through determining the concentration of unconsumed periodate after the oxidized reaction.<sup>[51]</sup> The 20% potassium iodide solution (2 mL) was added to the reaction mixture (5 mL) after it was neutralized by adding 10 mL of 10% sodium bicarbonate solution. The reaction was stirred in the dark at 25 °C for 30 min, and then the liberated iodine was titrated with standardized sodium thiosulphate solution (0.01 mol L<sup>-1</sup>) using starch (1%) as the indicator. The value of DO is 84.2%, which is averaged from triplicate oxidation experiments.

**Preparation of CEC-I-OSA-I-ADH Hydrogel:** The PBS solutions of OSA (10 wt%) were mixed with PBS solution containing CEC and ADH at different molar ratios ( $R = \text{M-NH}_2 : \text{M-CHO}$ ,  $\text{M-CHO} = \text{M-NH}_2 + \text{M-CONHNH}_2$ ) of 0, 0.2 0.5 0.8 1.0, respectively. The total weight

concentrations were set as 7.4 wt%. The mixture was mixed uniformly by vortex and eventually homogeneous hydrogels were obtained.

**FT-IR Spectra:** FT-IR spectra were recorded using FT-IR spectrometer (Nicolet 5700, Thermo Nicolet, USA). After OSA powder, CEC powder, dried OSA-I-ADH gel, and CEC-I-OSA-I-ADH gel ( $R = 0.5$ ) were compressed into films with KBr, the samples were tested.

**Rheological Measurements:** (1) The storage moduli ( $G'$ ) of CEC-I-OSA-I-ADH hydrogel disks (15 mm in diameter, 7.4 wt%) with different  $R$  (0, 0.2, 0.5, 0.8, and 1) were tested by rheometer fitted with parallel dentate antiskid plates (both upper and underside plates are 15 mm in diameter). Under a fixed strain level, 1.0%, the angular frequency was swept from 0.01 rad  $s^{-1}$  to 100 rad  $s^{-1}$ . (2) The CEC-I-OSA-I-ADH hydrogel disks (15 mm in diameter, 7.4 wt%) with  $R = 0.5$  was measured under strain amplitude sweep ( $\gamma = 10\%–800\%$ ) at a fixed angular frequency (10 rad  $s^{-1}$ ). (3) The alternate step strain sweep of CEC-I-OSA-I-ADH hydrogel disk (15 mm in diameter, 7.4 wt%) with  $R = 0.5$  was measured at a fixed angular frequency (10 rad  $s^{-1}$ ). Amplitude oscillatory strains were switched from small strain ( $\gamma = 1.0\%$ ) to subsequent large strain ( $\gamma = 80\%$ , 300%, and 800%) with 100 s for every strain interval. (4) Similar experiments were carried out for a fixed large strain ( $\gamma = 800\%$ ) with loading period changed from 100 to 300 s for each strain level.

**Macroscopic Self-Healing Experiments:** (1) Two pieces of  $R = 0.5$  CEC-I-OSA-I-ADH hydrogel disks (15 mm in diameter) stained by rhodamine B and methylene blue, were cut into equal 8 pieces, respectively. Then the total 16 pieces of alternate colors were alternate combined into two blended integral hydrogel disks, and were kept for 6 h at 25 °C. Then, the two healed hydrogel disks were immersed in PBS (pH 7.0) for 3 h for checking their stability. (2) Healing efficiency ( $HE$ ) of the CEC-I-OSA-I-ADH hydrogel ( $R = 0.2, 0.5, \text{ and } 0.8$ ) prepared in PBS (pH 7.0 and 6.0) was calculated by beam-shaped strain compression measurements. Two identical hydrogel samples were prepared as mentioned above. One of them was cut by razor and then healed for 12 h at 25 °C. Both the intact and the self-healed hydrogels were compressed by the beam-shaped mold until rupture occurred and the fracture strength of the intact ( $S_i$ ) and healed ( $S_h$ ) samples were recorded. Then the  $HE$  was calculated as  $S_h/S_i$ . The same compression experiment was used to determine the  $HE$  of CEC-I-OSA-I-ADH hydrogel ( $R = 0.5$ ) with different healing conditions (e.g., extending the healing time to 48 h, increasing the healing temperature to 37 °C).

**Injectable Model Drug Delivery System:** (1) The rhodamine B and methylene blue were used as two small molecular model drugs in this case. Two pieces of CEC-I-OSA-I-ADH hydrogel ( $R = 0.5$ ) disks (15 mm in diameter, 2  $cm^3$ ) containing rhodamine B (0.1  $mg\ cm^{-3}$ ) and methylene blue (0.1  $mg\ cm^{-3}$ ) were prepared, respectively. Then, the hydrogels incorporated different model drugs were separately immersed in 10 mL PBS (pH 7.0) at 25 °C. 1 mL of release medium was extracted 3 times at certain intervals for UV detection at 666 nm (methylene blue) and 554 nm (rhodamine B), and then replenished with 1 mL fresh PBS. (2) Two pieces of CEC-I-OSA-I-ADH hydrogel disks with two stains, rhodamine B and methylene blue, were synthesized as described above. They were separately put into two needles and then injected into a 10 mL small beaker. After compressing the hydrogel pieces in the bottom of the beaker and healing for 6 h at 25 °C, the self-healed hydrogel disk was immersed in 10 mL PBS (pH 7.0). Thereafter, the UV analyses were used to detect the release solutions by the above-mentioned approach.

**3D Cell Encapsulation and Cell Release:** The mouse NIH 3T3 fibroblasts were encapsulated in the CEC-I-OSA-I-ADH hydrogels ( $C_1 = 7.4\ wt\%$ ). The 3T3 cells were first suspended in the PBS solutions of OSA (10 wt%), and this cell suspension was then added into PBS mixture containing CEC and ADH ( $R = 0.5$ ). The cell loaded hydrogel (2.5 million cells  $mL^{-1}$ ) was formed within 20 s and incubated at 37 °C for 5 min. Thereafter, the cell loaded hydrogel was put into a 6-well tissue culture polystyrene dish containing 5 mL cell culture medium (DMEM containing 10% FBS) per well. The medium was changed after incubating 1 h at first time and then changed every 12 h. Cell viability was evaluated by Live/Dead staining after 12, 24, and 48 h, respectively. Incubating for 72 h, the hydrogel was partially degraded and the encapsulated cells were released from the culture medium. After centrifuged, 5 mL fresh medium was added

into the released cells for further cultivation. The cell morphology was monitored by phase contrast microscope (Olympus IX 71, Tokyo, Japan) after culturing for 3 days.

## Supporting Information

Supporting Information is available from the Wiley Online Library or from the author.

## Acknowledgements

This research was supported by National Natural Science Foundation of China (Grant Nos. 51173144 and 51073127) the Research Fund for the Doctoral Program of Higher Education of China, Scientific Research Foundation for the Returned Overseas Chinese Scholars, State Education Ministry, the Fundamental Research Funds for the Central Universities, International Science & Technology Cooperation Program Supported by Ministry of Science and Technology of China and Shaanxi Province (Grant No. 2013KW14-02), Key Innovational Research Team Program Supported by Shaanxi Province (Grant No. 2013KCT-05). Jinxiong Zhou acknowledges the financial support by NSFC through Grant Nos. 11372239, 11472210, and 11321062. Feng Xu was financially supported by the National Natural Science Foundation of China (Grant No. 11372243), the Key Project of Chinese Ministry of Education (Grant No. 313045), International Science & Technology Cooperation Program of China (Grant No. 2013DFG02930).

Received: May 8, 2014

Revised: September 17, 2014

Published online:

- [1] A. S. Hoffman, *Adv. Drug Delivery Rev.* **2012**, *64*, 18.
- [2] K. Y. Lee, D. J. Mooney, *Chem. Rev.* **2001**, *101*, 1869.
- [3] F. Xu, C. A. M. Wu, V. Rengarajan, T. D. Finley, H. O. Keles, Y. Sung, B. Li, U. A. Gurkan, U. Demirci, *Adv. Mater.* **2011**, *23*, 4254.
- [4] Y. M. Chen, Z. Q. Liu, Z. H. Feng, F. Xu, J. K. Liu, *J. Biomed. Mater. Res. A* **2013**, *102*, 2258.
- [5] Y. L. Han, Y. Yang, S. Liu, J. Wu, Y. M. Chen, T. J. Lu, F. Xu, *Biofabrication* **2013**, *5*, 35004.
- [6] Y. M. Chen, K. Dong, Z. Liu, F. Xu, *Sci. China Technol. Sc.* **2012**, *55*, 2241.
- [7] G. Y. Huang, L. Wang, S. Wang, Y. L. Han, J. Wu, Q. Zhang, F. Xu, T. J. Lu, *Biofabrication* **2012**, *4*, 42001.
- [8] M. C. Cushing, K. S. Anseth, *Science* **2007**, *316*, 1133.
- [9] a) S. Burattini, B. W. Greenland, D. Chappell, H. M. Colquhoun, W. Hayes, *Chem. Soc. Rev.* **2010**, *39*, 1973; b) Z. Wei, J. H. Yang, J. Zhou, F. Xu, M. Zrinyi, P. H. Dussault, Y. Osada, Y. M. Chen, *Chem. Soc. Rev.* **2014**, *43*, 8114.
- [10] J. A. Syrett, C. R. Becer, D. M. Haddleton, *Polym. Chem.* **2010**, *1*, 978.
- [11] R. P. Wool, *Soft Matter* **2008**, *4*, 400.
- [12] S. C. Li, P. Han, H. P. Xu, *Prog. Chem.* **2012**, *24*, 1346.
- [13] D. Y. Wu, S. Meure, D. Solomon, *Prog. Polym. Sci.* **2008**, *33*, 479.
- [14] S. J. Rowan, S. J. Cantrill, G. R. Cousins, J. K. Sanders, J. F. Stoddart, *Angew. Chem., Int. Ed.* **2002**, *41*, 898.
- [15] J. M. Lehn, *Chem. Soc. Rev.* **2007**, *36*, 151.
- [16] T. Maeda, H. Otsuka, A. Takahara, *Prog. Polym. Sci.* **2009**, *34*, 581.
- [17] J. M. Lehn, *Prog. Polym. Sci.* **2005**, *30*, 814.
- [18] D. C. Tuncaboylu, M. Sahin, A. Argun, W. Oppermann, O. Okay, *Macromolecules* **2012**, *45*, 1991.
- [19] Z. Rao, M. Inoue, M. Matsuda, T. Taguchi, *Colloids Surf., B* **2011**, *82*, 196.

- [20] G. Akay, A. Hassan-Raeisi, D. C. Tuncaboylu, N. Orakdogan, S. Abdurrahmanoglu, W. Oppermann, O. Okay, *Soft Matter* **2013**, *9*, 2254.
- [21] J. X. Cui, A. Del Campo, *Chem. Commun.* **2012**, *48*, 9302.
- [22] A. Phadke, C. Zhang, B. Arman, C. Hsu, R. A. Mashelkar, A. K. Lele, M. J. Tauber, G. Arya, S. Varghese, *Proc. Natl. Acad. Sci. U.S.A.* **2012**, *109*, 4383.
- [23] T. Kakuta, Y. Takashima, M. Nakahata, M. Otsubo, H. Yamaguchi, A. Harada, *Adv. Mater.* **2013**, *25*, 2849.
- [24] M. Nakahata, Y. Takashima, H. Yamaguchi, A. Harada, *Nat. Commun.* **2011**, *2*, 511.
- [25] M. M. Zhang, D. H. Xu, X. Z. Yan, J. Z. Chen, S. Y. Dong, B. Zheng, F. H. Huang, *Angew. Chem., Int. Ed.* **2012**, *51*, 7011.
- [26] Q. Wang, J. L. Mynar, M. Yoshida, E. Lee, M. Lee, K. Okuro, K. Kinbara, T. Aida, *Nature* **2010**, *463*, 339.
- [27] K. Haraguchi, K. Uyama, H. Tanimoto, *Macromol. Rapid Commun.* **2011**, *32*, 1253.
- [28] J. Liu, G. Song, C. He, H. Wang, *Macromol. Rapid Commun.* **2013**, *12*, 1002.
- [29] G. H. Deng, C. M. Tang, F. Y. Li, H. F. Jiang, Y. M. Chen, *Macromolecules* **2010**, *43*, 1191.
- [30] M. C. Roberts, M. C. Hanson, A. P. Massey, E. A. Karren, P. F. Kiser, *Adv. Mater.* **2007**, *19*, 2503.
- [31] L. H. He, D. E. Fullenkamp, J. G. Rivera, P. B. Messersmith, *Chem. Commun.* **2011**, *47*, 7497.
- [32] J. I. Jay, K. Langheinrich, M. C. Hanson, A. Mahalingam, P. F. Kiser, *Soft Matter* **2011**, *7*, 5826.
- [33] F. Y. Liu, F. Y. Li, G. H. Deng, Y. M. Chen, B. Q. Zhang, J. Zhang, C. Y. Liu, *Macromolecules* **2012**, *45*, 1636.
- [34] G. H. Deng, F. Y. Li, H. X. Yu, F. Y. Liu, C. Y. Liu, W. X. Sun, H. F. Jiang, Y. M. Chen, *ACS Macro Lett.* **2012**, *1*, 275.
- [35] J. A. Yoon, J. Kamada, K. Koynov, J. Mohin, R. Nicolaÿ, Y. Zhang, A. C. Balazs, T. Kowalewski, K. Matyjaszewski, *Macromolecules* **2011**, *45*, 142.
- [36] M. Pepels, I. Filot, B. Klumperman, H. Goossens, *Polym. Chem.* **2013**, *4*, 4955.
- [37] A. A. Kavitha, N. K. Singha, *ACS Appl. Mater. Interfaces* **2009**, *1*, 1427.
- [38] Z. Wei, J. H. Yang, X. J. Du, F. Xu, M. Zrinyi, Y. Osada, F. Li, Y. M. Chen, *Macromol. Rapid Commun.* **2013**, *34*, 1464.
- [39] P. Reutenauer, E. Buhler, P. J. Boul, S. J. Candau, J. M. Lehn, *Chem.-Eur. J.* **2009**, *15*, 1893.
- [40] K. Y. Lee, K. H. Bouhadir, D. J. Mooney, *Biomaterials* **2004**, *25*, 2461.
- [41] T. Boonthekul, H. Kong, D. J. Mooney, *Biomaterials* **2005**, *26*, 2455.
- [42] C. Le Tien, M. Millette, M. Lacroix, M. A. Mateescu, *Biotechnol. Appl. Biochem.* **2004**, *39*, 189.
- [43] R. S. Greenfield, T. Kaneko, A. Daues, M. A. Edson, K. A. Fitzgerald, L. J. Olech, J. A. Grattan, G. L. Spitalny, G. R. Braslawsky, *Cancer Res.* **1990**, *50*, 6600.
- [44] K. L. Tan, E. N. Jacobsen, *Angew. Chem., Int. Ed.* **2007**, *46*, 1315.
- [45] A. Herrmann, *Chem. Soc. Rev.* **2014**, *43*, 1899.
- [46] D. E. Apostolides, C. S. Patrickios, E. Leontidis, M. Kushnir, C. Wesdemiotis, *Polym. Int.* **2014**, *9*, 1558.
- [47] J. Yu, H. Deng, F. Xie, W. Chen, B. Zhu, Q. Xu, *Biomaterials* **2014**, *9*, 3132.
- [48] Y. L. Zhang, B. Yang, X. Y. Zhang, L. X. Xu, L. Tao, S. X. Li, Y. Wei, *Chem. Commun.* **2012**, *48*, 9305.
- [49] B. Yang, Y. L. Zhang, X. Y. Zhang, L. Tao, S. X. Li, Y. Wei, *Polym. Chem.* **2012**, *3*, 3235.
- [50] Y. L. Zhang, L. Tao, S. X. Li, Y. Wei, *Biomacromolecules* **2011**, *12*, 2894.
- [51] B. Balakrishnan, A. Jayakrishnan, *Biomaterials* **2005**, *26*, 3941.
- [52] K. H. Bouhadir, D. S. Hausman, D. J. Mooney, *Polymer* **1999**, *40*, 3575.
- [53] H. Jiang, Y. Wang, Q. Huang, Y. Li, C. Xu, K. Zhu, W. Chen, *Macromol. Biosci.* **2005**, *5*, 1226.
- [54] H. Sashiwa, N. Yamamori, Y. Ichinose, J. Sunamoto, S. I. Aiba, *Macromol. Biosci.* **2003**, *3*, 231.
- [55] H. Sashiwa, N. Yamamori, Y. Ichinose, J. Sunamoto, S. Aiba, *Biomacromolecules* **2003**, *4*, 1250.
- [56] T. Ono, S. Fujii, T. Nobori, J. Lehn, *Chem. Commun.* **2007**, 4360.
- [57] Y. Chiu, S. Chen, C. Su, C. Hsiao, Y. Chen, H. Chen, H. Sung, *Biomaterials* **2009**, *30*, 4877.
- [58] L. Haines-Butterick, K. Rajagopal, M. Branco, D. Salick, R. Rughani, M. Pilarz, M. S. Lamm, D. J. Pochan, J. P. Schneider, *Proc. Natl. Acad. Sci. U.S.A.* **2007**, *104*, 7791.
- [59] E. A. Appel, J. Del Barrio, X. J. Loh, O. A. Scherman, *Chem. Soc. Rev.* **2012**, *41*, 6195.
- [60] J. L. Vanderhooft, B. K. Mann, G. D. Prestwich, *Biomacromolecules* **2007**, *8*, 2883.